Astron. Astrophys. 347, 876–890 (1999)

ASTRONOMY AND ASTROPHYSICS

Testing convection theories using Balmer line profiles of A, F, and G stars*

R.B. Gardiner[1], **F. Kupka**[2], **and B. Smalley**[1]

[1] Department of Physics, Keele University, Keele, Staffordshire, ST5 5BG, UK (rbg,bs@astro.keele.ac.uk)
[2] Institute for Astronomy, University of Vienna, Türkenschanzstr. 17, A-1180 Vienna, Austria (kupka@astro.univie.ac.at)

Received 25 February 1999 / Accepted 26 May 1999

Abstract. We consider the effects of convection on the Balmer line profiles (H_α and H_β) of A, F, and G stars. The standard mixing-length theory (MLT) ATLAS9 models of Kurucz (1993), with and without overshooting, are compared to ATLAS9 models based on the turbulent convection theory proposed by Canuto & Mazzitelli (1991, 1992) and implemented by Kupka (1996), and the improved version of this model proposed by Canuto et al. (1996) also implemented by Kupka.

The Balmer line profiles are a useful tool in investigating convection because they are very sensitive to the parameters of convection used in the stellar atmosphere codes. The H_α and H_β lines are formed at different depths in the atmosphere. The H_α line is formed just above the convection zone. The H_β line, however, is partially formed inside the convection zone.

We have calculated the $T_{\rm eff}$ of observed stars by fitting Balmer line profiles to synthetic spectra and compared this to: (i) the $T_{\rm eff}$ of the fundamental stars; (ii) the $T_{\rm eff}$ of stars determined by the Infra-Red Flux Method and (iii) the $T_{\rm eff}$ determined by Geneva photometry for the stars in the Hyades cluster.

We find that the results from the H_α and H_β lines are different, as expected, due to the differing levels of formation. The tests are inconclusive between three of the four models; MLT with no overshooting, CM and CGM models, which all give results in reasonable agreement with fundamental values. The results indicate that for the MLT theory with no overshooting it is necessary to set the mixing length parameter α equal to 0.5 for stars with $T_{\rm eff} \leq 6000$ K or $T_{\rm eff} \geq 7000$ K. However for stars with 6000 K$\leq T_{\rm eff} \leq 7000$ K the required value for the parameter is $\alpha \geq 1.25$. Models with overshooting are found to be clearly discrepant, consistent with the results with $uvby$ photometry by Smalley & Kupka (1997).

Key words: convection – line: profiles – stars: atmospheres – stars: fundamental parameters – stars: interiors

1. Introduction

In stars later than mid A-type, convection can have a significant effect on the Balmer lines profiles. Thus our treatment of convection used in modelling the stellar atmosphere can alter interpretation of the observed profiles. Convection in the ATLAS code (Kurucz 1970) has always been included using the mixing-length theory (MLT) with modifications, the last one being 'approximate overshooting', as discussed by Castelli (1996). The more recently developed CM theory (Canuto & Mazzitelli 1991, 1992) proposes a model with a full spectrum turbulence as an improvement to the one-eddy MLT model.

Changing convective flux can easily make large changes in the model colours, as discussed in Smalley & Kupka (1997; hereafter Paper I). In Paper I, comparison with fundamental $T_{\rm eff}$ and log g revealed that the CM model gave results that were generally superior to the standard MLT without overshooting with α=1.25, the mixing length parameter adopted in Kurucz's grids. They found MLT with overshooting models to be discrepant.

In this work we present a discussion of the effects of different treatments of convection on the H_α and H_β profiles.

We have considered four models of convection: the standard mixing-length theory ATLAS9 models of Kurucz (1993), with and without approximate overshooting, with values of mixing length parameter α=1.25 and 0.5; ATLAS9 models with the turbulent convection theory proposed by Canuto & Mazzitelli (1991, 1992) and implemented by Kupka (1996) and an improved version proposed by Canuto et al. (1996) also implemented by Kupka. Six grids of solar-metallicity synthetic spectra in the region of H_α and H_β lines were computed (one for each convection model). The spectra were fitted to the observations to derive $T_{\rm eff}$, after having fixed log g.

We have compared the $T_{\rm eff}$ obtained by these models to (i) the $T_{\rm eff}$ of the fundamental stars discussed by Smalley & Dworetsky (1995) and Smalley (1999); (ii) the $T_{\rm eff}$ of stars determined by the Infra-Red Flux Method presented by Blackwell & Lynas-Gray (1994) and (iii) the $T_{\rm eff}$ determined by Geneva photometry, as calibrated by Künzli et al. (1997) for the stars in the Hyades cluster.

Send offprint requests to: Rebecca Gardiner

* Based on observations made at the Observatorio del Roque de los Muchachos using the Richardson-Brealey Spectrograph on the 1.0m Jacobs Kapteyn Telescope.

2. Observations and reduction

The spectroscopic observations were made at the Observatorio del Roque de los Muchachos, La Palma using the Richardson-Brealey Spectrograph on the 1.0m Jacobus Kapteyn Telescope (JKT) in 1997 October/November. A 2400 l mm^{-1} holographic grating was used and a 1124 × 1124 pixel Tek CCD, giving a resolution of 0.4Å FWHM. Nearly 250 observations of H_α line profiles were taken and 50 H_β line profiles, with associated calibration files.

The data reduction was performed using the Starlink ECHOMOP software package (Mills et al. 1997). The spectra generally had a signal-to-noise ratio in excess of 100:1. The wavelength of the Balmer core, was in each spectrum, shifted to the laboratory value of 6562.797 Å for H_α and 4861.332 Å for H_β, to correct for radial velocity shifts.

It is important that the true shape of the profile is preserved in the reduction (Smith & van't Veer 1987). Instrumental sensitivity variations were removed by comparing to observations of stars with intrinsically narrow Balmer profiles, for example early-B or O type stars and G type stars. The spectra were rectified at both ± 40 Å and ± 100 Å and both regions were fitted to synthetic spectra. They gave the same result. The profiles for Vega were in excellent agreement with those of Peterson (1969) and the H_β profile for Procyon was almost identical to that observed and reduced by van't Veer-Menneret & Megessier (1996) after resolutions were matched. The observations of the Sun used in this paper are from Kurucz et al. (1984).

3. Models and Balmer profiles

In Smalley & Kupka (1997) it was found that changing convective flux in model atmospheres makes large changes to the model colours. They considered the CM model and MLT models (using α=1.25) with and without overshooting. The CM model performed best in predicting $T_{\rm eff}$ and log g of fundamental and non-fundamental stars. Also the MLT model without overshooting gave reasonable results within the error bars. MLT models with overshooting however gave very poor results and was thus ruled out as a sufficiently accurate theory of conditions in stellar atmospheres. In this work, six grids of model atmospheres have been computed.

In the ATLAS6 (Kurucz 1979b) models, the mixing length theory was introduced. This theory is a phenomenological approach to convection in which it is assumed that one eddy ("bubble"), which has a given size as a function of local mixing length, transports all of the convective energy. One of the short-comings of MLT is that it has an adjustable parameter α being the scale height that a hot bubble rises in the atmosphere before dissipating its heat to the surrounding gases. The value of α has changed in the several ATLAS versions, and in ATLAS9, α was assumed to be 1.25 to fit the energy distribution from the centre of the Sun. The parameter α has had to be set at differing values to fit different types of observations (Steffen & Ludwig 1999), no single value working in all cases. For the Sun and other stars, van't Veer-Menneret & Megessier (1996) found that setting α = 0.5 fits best overall when looking at the first four line profiles in the Balmer series. So for this work separate grids were calculated for the two values of α=1.25 and 0.5.

In ATLAS9 (Kurucz 1993), a horizontally averaged opacity and an "approximate overshooting" were included. This approximate overshooting is based on smoothing the convective flux over a certain fraction of the local pressure scale height at the transition between stable and unstable stratification (see Castelli et al. 1997). It yields a positive mean convective flux right at the beginning of the stable stratification. Again we computed two grids of model atmospheres using mixing length theory with overshooting; one with α = 1.25, one with α = 0.5.

A turbulent theory of convection was proposed by Canuto & Mazzitelli (1991, 1992) which accounts for eddies of a full range of sizes and which interact with each other. The mixing length used is taken to be the distance to the nearest stable layer, $l = z$. Thus the CM model corrects the MLT "one-eddy" approximation and has no adjustable free parameters, unlike MLT in which α could be adjusted to fit observations. The CGM model was proposed in Canuto et al. (1996), as an improvement to the CM model. It differs from the CM model in that the rate of energy input $n_s(k)$ is controlled by both the source and the turbulence it generates. However the representation of the non-linear interactions used had to be less complete than the one in the CM model, in order that the equations could still be solved numerically.

Thus the six grids computed using solar-metallicity Kurucz (1993) ATLAS9 models, for values of $T_{\rm eff}$ between 5500 K and 9750 K in steps of 250 K and values of log g between 3.50 and 5.0 in steps of 0.5, identical except for the theory of convection in each case are as follows:

1. Standard ATLAS9 models using mixing length without convective overshooting. The value of the mixing length parameter α is the standard value of 1.25. These will be referred to as MLT_noOV(α=1.25) models in this paper.
2. Standard ATLAS9 models using mixing length without convective overshooting. The value of the mixing length parameter α is 0.5. These will be referred to as MLT_noOV(α=0.5) models.
3. Standard ATLAS9 models using mixing length with approximate overshooting. The value of the mixing length parameter α used is 1.25. These will be referred to as MLT_OV(α=1.25) models.
4. Standard ATLAS9 models using mixing length with approximate convective overshooting. The value of the mixing length parameter α used is 0.5. These will be referred to as MLT_OV(α=0.5) models.
5. Modified ATLAS9 models using the Canuto & Mazzitelli (1991, 1992) model of turbulent convection. These will be referred to as the CM models.
6. Modified ATLAS9 models using the Canuto et al. (1996) model of turbulent convection. The value used for the parameter $\alpha-$CGM is 0.09 (refer to Canuto et al. 1996 for definition of this parameter). These will be referred to as the CGM models.

The grids of synthetic spectra were calculated using UCLSYN (Smith 1992, Smalley & Smith 1995) which includes Balmer line profiles calculated using the Stark-broadening tables of Vidal et al. (1973) and metal absorption lines from the Kurucz & Bell (1995) linelist. This routine is based on the BALMER routine (Peterson 1969, Kurucz 1993) which includes resonance and Van der Waals broadening. The spectra were rotationally broadened as necessary and instrumental broadening was applied with $\mathrm{FWHM} = 0.4$ Å to match the resolution of the observations. The synthetic spectra were normalised at ± 40 Å and ± 100 Å to match the observations. The values of $T_{\rm eff}$ were obtained by fitting model profiles to the observations using the least-square differences. The results given in this paper are using observations and model profiles normalised at ± 100 Å, although the results are not significantly different using normalisation at ± 40 Å. A microturbulence of 2 kms^{-1} was assumed throughout for both the model atmosphere line opacities and spectrum synthesis.

High rotation and metallicity causes difficulties in modelling both Balmer line profiles and may be part of the systematic problems with the profiles, although these would be expected to effect H_β more than H_α as there are more metal lines in this wavelength region. The values of $v \sin i$ included in the tables are from Bernacca & Perinotto (1970). Values of metallicity are given in the tables, using the δm_0 calibrations, derived by Nissen (1988), Berthet (1990) and Smalley (1992). These calibrations are model-dependent and thus not definitive. The $uvby\beta$ data was taken from Hauck & Mermilliod (1998). The results presented for $T_{\rm eff}$ are not very influenced by poor agreement of metal lines as even at high values of $v \sin i$ the hydrogen line profile itself is not broadened significantly. Thus as the observations were fitted visually it was clear that the metal lines were stronger when looking at a star with high metal abundances. As a check in several cases model profiles were generated with higher metal abundances, at the same $T_{\rm eff}$ as one interpolated from the grids, and compared. The resulting fits to H_α observations were affected by $\leq$50 K (a decrease in calculated $T_{\rm eff}$) for an increase in metal abundance of 0.1 dex. The H_β line was affected more than H_α profile, but still the effect is $\leq$50 K for values of $T_{\rm eff} \geq 6500$ K and around 50–75 K for $5500\,\mathrm{K} \leq T_{\rm eff} \leq 6500$ K. Thus the fit is not significantly affected by using solar metallicity grids, provided that the metallicity uncertainty is on the order of $\pm$0.1 dex.

Model H_α or H_β profiles for a particular $T_{\rm eff}$, given log g, were obtained by interpolation between the four closest places on the grid either side of the required value of $T_{\rm eff}$ and log g.

The H_α and H_β profiles generated using the six different convection theories for a given $T_{\rm eff}$ and log g are all visually clearly different, for all values of $T_{\rm eff}$ below 8500 K (see Fig. 1). Fig. 1 shows profiles at 7000 K as an example but the trends between models are the same at all values of $T_{\rm eff}$. Fig. 2 (left) shows the temperature structure in synthesized stars using the different convection models and (right) shows the average optical depth of the peak of the contribution function (as defined by Gray 1992) of all points on the H_α and H_β line profiles for these models.

The Balmer lines are very sensitive to the parameters of convection used in the stellar atmosphere codes since the treatment of convection can dramatically alter the temperature structure at the depths where the lines are formed. For example, for a star of $T_{\rm eff} = 7000\ K$ the MLT_noOV model with α=1.25 has a significant fraction of convective to radiative flux at depths $\tau \geq$ 0.05, and the temperature structure above this depth is effected by this convection zone. Thus although the average depth of formation of the two Balmer lines are not within this convection zone as can be seen in Fig. 2 (right), they are affected by the different temperature structures in the region where they are formed. In the case of MLT_noOV the H_β profile is affected more by the choice of the mixing-length parameter α than the H_α profile since it is formed closer to the unstable region. In the MLT_OV model of the same $T_{\rm eff}$ there is significant fraction of convective flux between -0.53$\leq \tau \leq$ 1.8. Thus both Balmer profiles are considerably affected by whether approximate overshooting is assumed or not. For H_α, the MLT_noOV and the CM results are close because the models give very similar conditions (ie. temperatures, pressure) in all layers above the convection zone where H_α is formed. Between 6000 and 8000 K, in the MLT_OV, the convection zone extends into the region where the H_α profile is formed and gives higher temperatures with a lower gradient in this region. The profile is formed over a smaller range of depths between 40–100Å, but then relative to this there occurs a large change in depth of formation closer to the core. This causes the synthesized profiles to become narrower given a specified $T_{\rm eff}$. Thus, the MLT_OV profile which matches any observed profile is always one of a higher effective temperature.

For H_β, the profile is formed nearer or in the convective zone for all models, at all temperatures where the convection zone has an influence on the temperature structure of the atmosphere, that is for stars with $T_{\rm eff} \leq$ 8500 K. MLT_noOV(α=1.25) and CM give different results because the points on the CM profile are formed over a more gradual change in depth and temperature in the atmosphere, thus giving a broader profile for a given $T_{\rm eff}$. Therefore, the CM model which matches any observed profile is always one of a lower $T_{\rm eff}$. The MLT_noOV(α=1.25) H_β profiles are formed higher in the convection zone at a slightly cooler region. However, Fig. 1 shows that not only does this mean that the effective temperature of the MLT_noOV(α=1.25) profile which matches the CM profile at 7000 K closest is higher by $\sim$250 K, but also, and very significantly, it has a different shape. However setting the parameter α=0.5 in the MLT_noOV model predicts conditions much more similar to those of the CM model than using the standard value α=1.25.

For $T_{\rm eff} \geq 8500\ K$ convection in all the theories we are looking at become so insignificant as to not effect results. The Balmer line profiles are virtually insensitive to log g below $\sim$ $8000\ K$ thus any errors in the values of log g used will not effect the results.

The errors in determining $T_{\rm eff}$ by fitting a model Balmer line profile to observations are all of the order of 100 K below 8000 K, but increase to around 200 K by 8500 K. This error must then be combined with errors in the fundamental values of $T_{\rm eff}$ in order to get the error in $\Delta T_{\rm eff}$. Above 8000 K the Balmer profiles

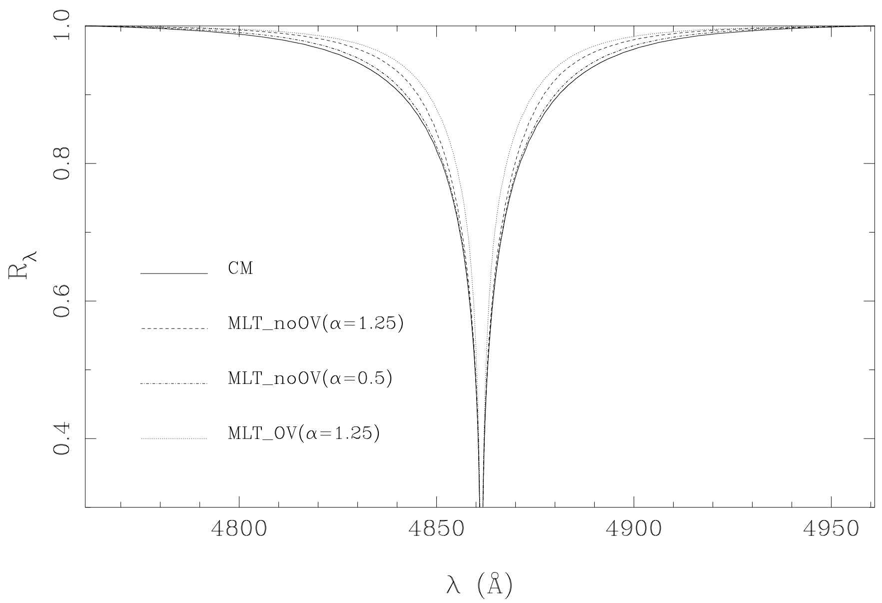

Fig. 1. The residual flux (R_λ) for the synthesised H_β profile for the CM, MLT_noOV(with $\alpha = 1.25$ and $\alpha = 0.5$) and MLT_OV($\alpha = 1.25$ only) models at 7000 K and log$g$ 4.0. The MLT_OV($\alpha = 0.5$) model is omitted for clarity but it is very close to the MLT_noOV(with $\alpha = 1.25$) profile. Note that the CM model gives the broadest profile, and the MLT_noOV(with $\alpha = 0.5$) profile is very similar to the CM profile at this temperature. The MLT_noOV(with $\alpha = 1.25$) profile is considerably narrower, and the MLT_OV($\alpha = 1.25$) profile is even narrower.

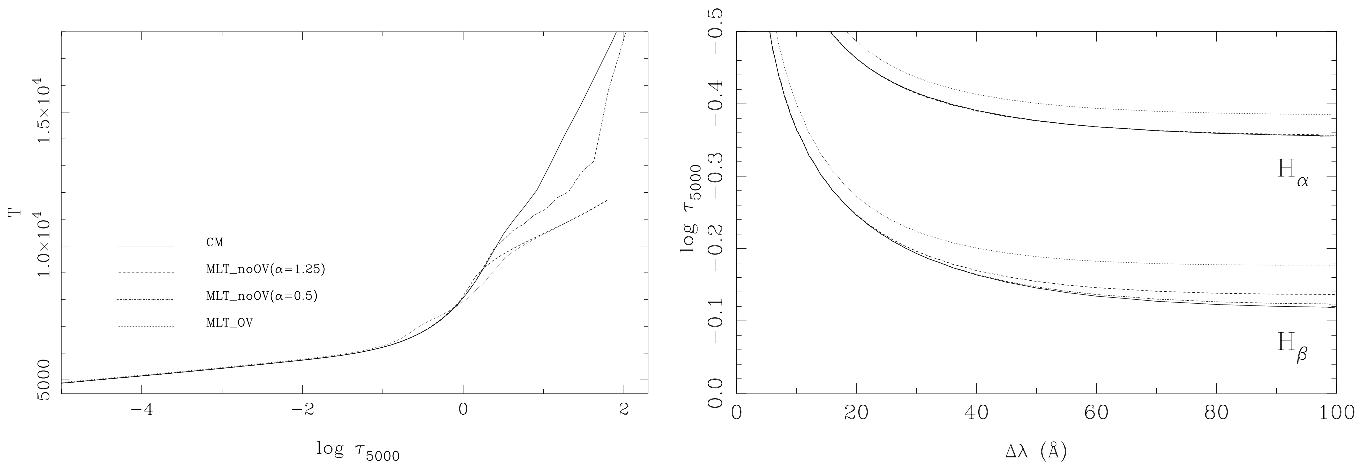

Fig. 2. (*Left*) Temperature shown against optical depth τ_{5000} for model atmosphere of $T_{\rm eff}$ 7000 K and log g 4.0. The solid line is the CM model, the dashed line is the MLT_noOV($\alpha = 1.25$), the dot-dashed line is MLT_noOV($\alpha = 0.5$) and the dotted line is MLT_OV($\alpha = 1.25$). (*Right*) Comparison between the optical depth of formation of each point on the Balmer profiles for each model atmosphere of $T_{\rm eff}$ 7000 K and log g 4.0. Note for H_α the depth of formation is very close for the CM and MLT_noOV models. However MLT_OV is formed much higher in the atmosphere in the wings 20 – 100Å and the decrease of depth of formation is gradual in the wings but then sharply increases towards the core. Thus MLT_OV is characterised by narrower profiles (as seen above in Fig. 1). The H_β profile at 100Å for CM is formed significantly deeper in the atmosphere than the MLT_noOV($\alpha = 1.25$) profile and the depth varies more gradually with distance from the core. Thus when normalised at 100Å the CM has a broader profile as it is formed over a larger variation of temperatures (again as seen in Fig. 1.)

become sensitive to log g (Gray 1992) making it important to have a fundamental value of log g with a small error. At 8000 K, a change in assumed log g of 0.25 for a particular star would have an equivalent effect to changing the temperature of the model profile an observation is fit to by ~150 K. For this reason and due to the problem found later of results being anonymously low compared to fundamental values, stars with $T_{\rm eff} \geq 8000$ K will be excluded from the statistical tests below.

4. $T_{\rm eff}$ from Balmer lines

We discuss the temperature derived from the six grids presented in the previous section. The $T_{\rm eff}$ was determined from the H_α and H_β profiles separately for each star, for each model and then compared with previously determined $T_{\rm eff}$ from other methods. We consider $T_{\rm eff}$ for fundamental stars (Smalley & Dworetsky 1995, Smalley 1999), $T_{\rm eff}$ from the Infra-Red Flux Method (Blackwell & Lynas-Gray 1994), and $T_{\rm eff}$ for the Hyades stars (Künzli et al. 1997).

As in Paper I, three statistical measures will be used to compare the four convection models:

1. A weighted mean of the differences between the value calculated from the Balmer line profile and the previously determined value as detailed in the introduction, in order to

determine which model is in closest overall agreement with the previous values.

2. A weighted root mean square of the differences, given by

$$rms = \sqrt{\frac{\sum \omega_i (\Delta x_i)^2}{\Sigma \omega_i}},$$

where ω_i are the weights as given by the square of the reciprocal of the errors, and Δx_i are the differences between the Balmer line-derived value and the value previously determined.

3. The reduced chi-square χ_v^2 and its associated probability, $P(\chi_v^2)$, as a measure of the goodness of agreement between the Balmer line-derived value and the value previously determined.

These three measures, together with a visual inspection of the figures, enable us to compare the four models.

4.1. Comparison with fundamental stars

The ideal test of the method of fitting observed profiles to model spectra is to compare the derived $T_{\rm eff}$ with direct model-independent methods. There are only 12 such fundamental stars in this temperature region, due to necessary observations being currently unavailable. The fundamental values were taken from Smalley & Dworetsky (1995) and Smalley (1999). Of these stars, Procyon (HD 61421) has the most tightly constrained value of $T_{\rm eff}$ due to the accuracy of the direct measurement of angular diameter. The four binary systems (HD16739, HD110379, HD185912, HD 202275) have larger errors due to the extra steps required to obtain the values of $T_{\rm eff}$ (Smalley 1999). Two stars, HD159561 and HD187642, do not have fundamental values of log g (see Smalley & Dworetsky 1995) and have high values of $v \sin i$.

The results are shown in Figs. 3 and 4, as a function of $\Delta T_{\rm eff}$ = $T_{\rm eff}$(Balmer) - $T_{\rm eff}$(fund) against $T_{\rm eff}$(fund), and in Tables 1 and 2. The results of the statistical tests are presented in Table 3. The large error bars are due to the uncertainties in the fundamental values. The error in fitting to a model Balmer line is combined with the error in the fundamental value to give the total error for $\Delta T_{\rm eff}$. Despite the small number of stars there is a trend which can be seen in the H_α results between ~ 6000–$9000\ K$, as temperature increases, the Balmer line method to give increasingly lower values of $T_{\rm eff}$ compared to the fundamental value. Above $\sim 8000\ K$ this slope becomes much steeper giving very low values for $T_{\rm eff}$ - up to 500 K lower than fundamental values. For stars with $T_{\rm eff} \geq$ 9000 K, where convection no longer has an effect on the profiles, the results return to being in close agreement with the fundamental values. The $T_{\rm eff}$ and log g of the Sun are known very precisely, those used by the Kurucz solar model are 5777 K and 4.4377 respectively (Kurucz 1992). The results in this paper for $T_{\rm eff}$ for the Sun from the H_β profile are in complete agreement with those found by van't Veer-Menneret & Megessier (1996) in which only MLT_noOV with α=0.5 fitted well at the known temperature 5777 K. The profiles generated using MLT_noOV with α=1.25 and MLT_OV model with either α=1.25 and 0.5 were considerably too narrow. Here, using the turbulence models (CM and CGM) the generated H_β profile also fits very well at the known temperature, in fact slightly better than MLT_noOV(α=0.5). However for the H_α profile, the turbulence models and the MLT_noOV models do not fit the observed profiles of the Sun at 5777 K. They fit at about ∼100 K lower. Only MLT_OV fits well at the correct temperature. These H_α results thus differ from those found by Castelli et al. (1997), who found that a no-overshooting model with α=1.25 fitted observations very well with no need to adjust α, and that models with overshooting had too weak a profile at 5777 K. Also the results differ from van't Veer-Menneret & Megessier (1996) and Fuhrmann et al. (1993) who both found that the best model was one without overshooting and α=0.5. The results between these three papers probably differ because of different continuum and line opacities and continuum levels.

Procyon has the most tightly constrained fundamental value of $T_{\rm eff}$ (6560±130 K) and thus gives the most insight into the accuracies of the four models. Fig. 3 shows that the H_α line profile results are in excellent agreement with the fundamental value for the CM, CGM and MLT without overshooting models, while the MLT with overshooting model result is 240 K higher than the fundamental one. For H_β the result using the CM model is 6325 K which is too low, the MLT_noOV(α=1.25) is in good agreement, MLT_noOV(α=0.5) is 249 K too low and the MLT_OV is again too high at 6789 K.

For the fundamental stars H_α profiles, the MLT_noOV ($\alpha = 1.25$) model gives the best agreement with fundamental values, giving a weighted mean difference of $-64 \pm 83\ K$ and a weighted root mean square difference of 109 K. However, the χ_v^2 is 0.70 which gives only a 62% probability that the model agrees with the fundamental values. Overall the MLT_noOV, CM and CGM models are all acceptable, but the MLT_OV models are discrepant with the given error bars. The H_β profiles also show the same order of success of the models, the best fit from MLT_noOV ($\alpha = 1.25$), with a 73% chance of agreement (χ_v^2 = 0.52). Again the MLT_OV model has an extremely poor fit with χ_v^2 of 4.27 giving less than a 1% chance of agreement. In general, fitting H_β profiles gives lower results for $T_{\rm eff}$ than from fitting to the H_α profile for $T_{\rm eff} \leq 7500\ K$ and slightly higher results for stars with $T_{\rm eff} \geq 7500\ K$. This is the case for all models and even over 9000 K when convection is insignificant. Thus it appears to be an inconsistency of the Balmer lines which is unrelated to convection.

Note, that the H_β profiles have larger errors associated with them, due to more metal lines in this region, making it slightly more difficult to fit observations to synthesised spectra. The H_β profiles can be seen to be more sensitive to mixing length than the H_α profiles, with a change in mixing length parameter from α=1.25 to α=0.5 causing the result for $T_{\rm eff}$ to decrease by around 200 K, compared to a decrease of only 50-100 K in results from the H_α profile. Over 7000 K setting α=0.5 reduces the difference between results from H_α and H_β. However for $6000\ K < T_{\rm eff} < 7000\ K$ setting α=0.5 tends to increase the difference between the results from the two lines, with H_β's results being on average ∼200 K lower than H_α's when us-

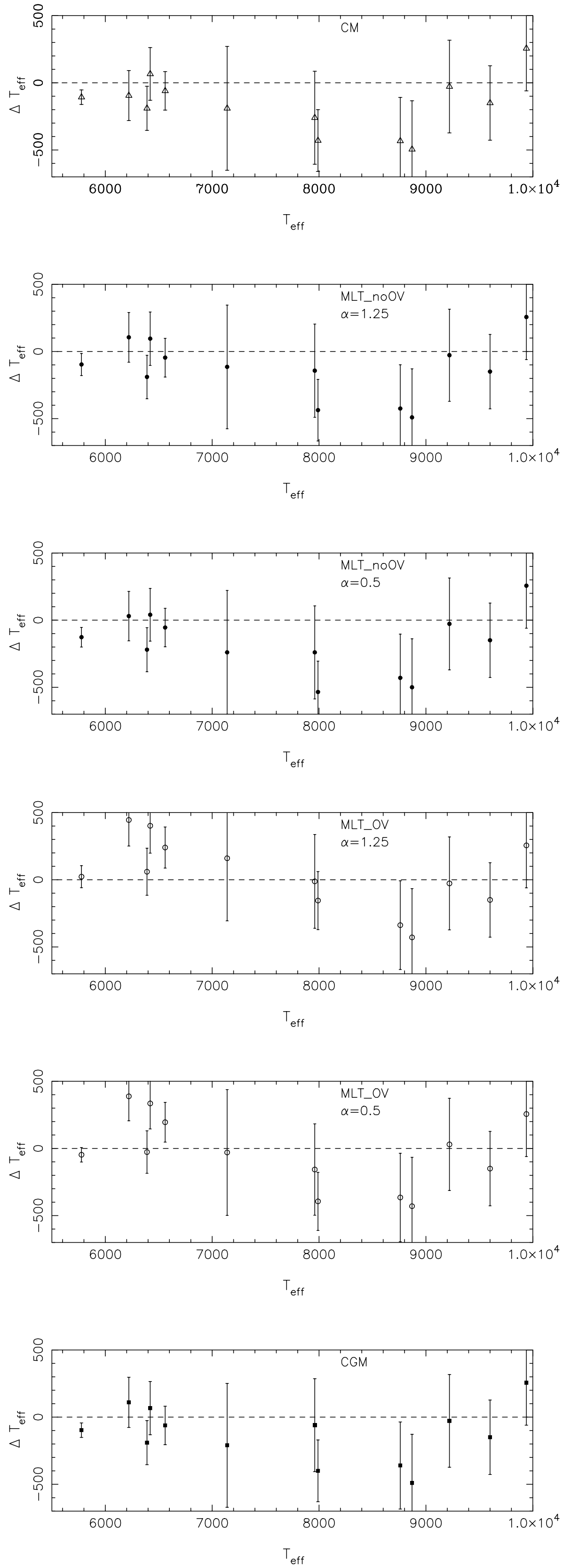

Fig. 3. Comparison between $T_{\rm eff}$ calculated from Balmer line profiles H_α to those derived from Fundamental methods for the four convection models showing the errors. $\Delta T_{\rm eff} = T_{\rm eff}(\rm Balmer) - T_{\rm eff}(\rm fund)$ is plotted against $T_{\rm eff}$(fund).

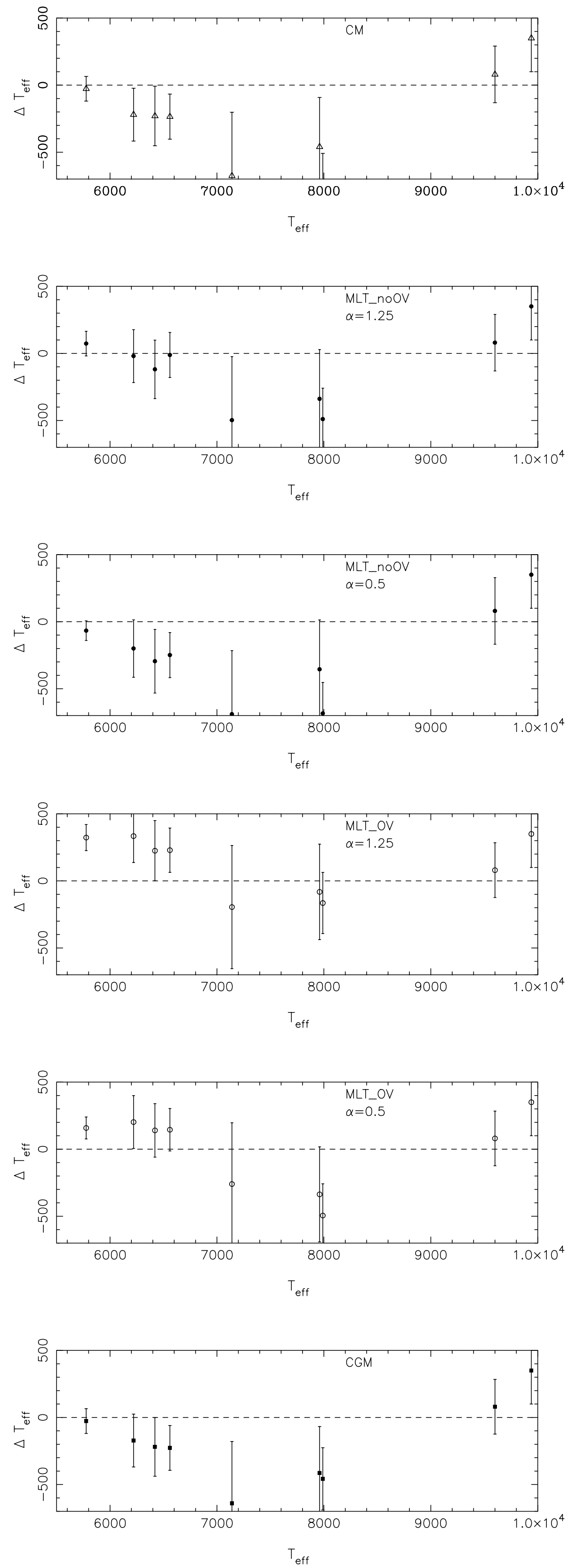

Fig. 4. Comparison between $T_{\rm eff}$ calculated from Balmer line profiles H_β to those derived from Fundamental methods for the four convection models showing the errors.

Table 1. $T_{\rm eff}$ for fundamental stars from H_α profiles

Fundamental					CM		MLT_noOV			
							α = 1.25		α = 0.5	
HD	$v\sin i$	[M/H]	$T_{\rm eff}$	$\log g$	$T_{\rm eff}$	$\Delta T_{\rm eff}$	$T_{\rm eff}$	$\Delta T_{\rm eff}$	$T_{\rm eff}$	$\Delta T_{\rm eff}$
Sun	2	0.00	5777±20	4.44	5670±50	−107±54	5680±80	−97±82	5650±70	−127±73
16739	13	+0.33	6220±170	4.26	6125±75	−95±186	6325±73	105±185	6250±70	30±184
61421	3	+0.07	6560±130	4.06	6500±60	−60±143	6514±60	−46±144	6505±60	−55±143
48915	5	+0.09	9940±210	4.33	10196±236	256±316	10196±236	256±316	10196±236	256±316
110379	25	−0.05	7140±459	4.21	6950±100	−190±461	7025±96	−115±460	6900±100	−240±461
159561	240	−0.20	7960±330	3.80	7700±104	−260±346	7817±107	−143±347	7720±104	−240±346
172167	10	+0.09	9600±180	4.10	9450±210	−150±277	9450±210	−150±277	9450±210	−150±277
185912	50	+0.05	6420±180	4.33	6486±80	66±196	6515±85	95±199	6460±80	40±196
187642	245	−0.05	7990±210	4.20	7560±94	−430±230	7553±91	−437±229	7455±94	−535±230
202275	13	−0.20	6390±150	4.34	6200±66	−190±164	6200±61	−190±162	6170±66	−220±164
102647	122	+0.20	8870±350	4.10	8375±90	−495±361	8379±95	−491±362	8370±90	−500±361
216956	85	+0.20	8760±310	4.20	8327±95	−433±324	8335±100	−425±326	8330±100	−430±326
47105	48	+0.09	9220±330	3.50	9192±102	−28±345	9192±95	−28±343	9192±91	−28±342

	Fundamental	MLT_OV				CGM	
		α = 1.25		α = 0.5			
HD	$T_{\rm eff}$	$T_{\rm eff}$	$\Delta T_{\rm eff}$	$T_{\rm eff}$	$\Delta T_{\rm eff}$	$T_{\rm eff}$	$\Delta T_{\rm eff}$
Sun	5777±20	5800±80	23±82	5730±50	−47±54	5680±50	−97±54
16739	6220±170	6665±63	445±194	6608±65	388±182	6330±77	110±187
61421	6560±130	6800±81	240±153	6755±70	195±148	6498±60	−62±143
48915	9940±210	10196±236	256±316	10196±236	256±316	10196±236	256±316
110379	7140±459	7300±82	160±466	7110±90	−30±468	6930±100	−210±461
159561	7960±330	7948±113	−12±349	7803±83	−157±340	7900±104	−60±346
172167	9600±180	9450±210	−150±277	9450±210	−150±277	9450±210	−150±277
185912	6420±180	6822±96	402±204	6755±60	335±190	6487±83	67±198
187642	7990±210	7835±51	−155±216	7596±50	−394±216	7590±94	−400±230
202275	6390±150	6450±90	60±175	6363±50	−27±158	6200±66	−190±164
102647	8870±350	8441±98	−429±363	8440±99	−430±364	8380±95	−490±362
216956	8760±310	8422±114	−338±330	8395±110	−365±329	8400±95	−360±324
47105	9220±330	9193±105	−27±346	9250±95	30±343	9192±102	−28±345

ing α=0.5, compared to being only $\sim 100\ K$ lower using the standard α=1.25.

Due to the trend already noted in the H_α results between $\sim$ 6000 and $\sim$ 9000 K as temperature increases, where the Balmer line method gives increasingly lower values of the Fundamental value, the statistics can not really represent performance indicators and may be misleading.

4.2. Comparison with IRFM stars

Due to the lack of truly fundamental stars, non-fundamental stars have to be used. However, these can introduce systematic errors. The Infrared Flux Method (IRFM) developed by Blackwell & Shallis (1977) uses model atmospheres only to determine the stellar surface infrared flux, but this is relatively insensitive to the actual model atmosphere. Thus the IRFM method can almost be considered as model independent, and thus semi-fundamental. Unfortunately due to lack of Balmer-line observations, there are relatively few stars with IRFM values of $T_{\rm eff}$ considered here. The results are shown in Figs. 5 and 6 and Tables 4 and 5.

For the H_α profiles IRFM stars, the MLT_noOV model gives values of $T_{\rm eff}$ which agree best with those given by the IRFM.

Considering the H_β profile results for the IRFM stars MLT_OV($\alpha = 0.5$) has the best agreement and MLT_noOV ($\alpha = 1.25$) is also in very good agreement.

4.3. Comparison with Hyades stars

In order to identify trends, the stars in the Hyades cluster were used, with the values of $T_{\rm eff}$ determined by Geneva photometry (Künzli et al. 1997), which estimated $T_{\rm eff}$ from the previous calibration of Kobi & North (1990). The $T_{\rm eff}$s of the Hyades are thus based on an old calibration based on Kurucz models which did not include molecular opacity, and used the mixing-length theory. Thus the comparisons in this section will not show which convection model is the correct one and thus is not as useful as comparing to fundamental or IRFM values. However, it is still instructive to compare to a method independent to ours, especially as the results show the same trend as the fundamental stars in Sect. 4.1, and molecular opacity in any case only affects the stars at the very left of the diagrams around $T_{\rm eff} \leq 6500\ K$.

Table 2. $T_{\rm eff}$ for fundamental stars from H_β profiles

Fundamental					CM		MLT_noOV			
							α = 1.25		α = 0.5	
HD	$v \sin i$	[M/H]	$T_{\rm eff}$	$\log g$	$T_{\rm eff}$	$\Delta T_{\rm eff}$	$T_{\rm eff}$	$\Delta T_{\rm eff}$	$T_{\rm eff}$	$\Delta T_{\rm eff}$
Sun	2	0.00	5777±20	4.44	5750±90	−27±92	5850±90	73 ±92	5710±70	−67±73
16739	13	+0.33	6220±170	4.26	6000±100	−220±197	6200±100	−20±197	6020±130	−200±214
48915	5	+0.09	9940±210	4.33	10290±135	350±250	10290±135	350±250	10290±135	350±250
61421	3	+0.07	6560±130	4.06	6325±106	−235±168	6548±106	−12±168	6311±107	−249±168
110379	25	−0.05	7140±450	4.21	6464±150	−676±474	6642±150	−498±474	6450±150	−690±474
159561	240	−0.20	7960±330	3.80	7500±165	−460±368	7621±165	−339±368	7605±165	−355±368
172167	10	+0.09	9600±180	4.10	9680±110	80±211	9520±110	80±211	9680±170	80±248
185912	50	+0.05	6420±180	4.33	6190±130	−230±222	6301±123	−119±218	6125±155	−295±237
187642	245	−0.05	7990±210	4.20	7250±96	−740±231	7500±96	−490±231	7306±96	−684±231

	Fundamental	MLT_OV				CGM	
		α = 1.25		α = 0.5			
HD	$T_{\rm eff}$	$T_{\rm eff}$	$\Delta T_{\rm eff}$	$T_{\rm eff}$	$\Delta T_{\rm eff}$	$T_{\rm eff}$	$\Delta T_{\rm eff}$
Sun	5777±20	6100±95	323±97	5935±80	158±82	5750±90	−27±92
16739	6220±170	6554±100	334±197	6422±100	202±197	6048±99	−172±197
48915	9940±210	10290±135	350±250	10290±135	350±250	10290±135	350±250
61421	6560±130	6789±102	229±165	6705±90	145±158	6333±105	−227±167
110379	7140±450	6945±92	−195±459	6880±80	-260±457	6500±100	−640±461
159561	7960±330	7878±136	−82±356	7623±130	-337±354	7546±105	−414±346
172167	9600±180	9680±95	80±204	9680±95	80±204	9680±95	80±204
185912	6420±180	6675±135	225±225	6560±85	140±199	6201±125	−219±219
187642	7990±210	7825±89	−165±228	7495±110	-495±237	7532±99	−458±232

Table 3. Statistics test results

	H_α					H_β				
	Weighted mean	Weighted rms	χ^2_v	n	% probability of good fit	Weighted mean	Weighted rms	χ^2_v	n	% probability of good fit
Fundamental										
CM	−100	111	1.20	6	31%	−122	177	1.60	5	16%
MLT_noOV($\alpha = 1.25$)	−64	109	0.70	6	62%	14	100	0.52	5	73%
MLT_noOV($\alpha = 0.5$)	−102	126	1.06	6	38%	−128	168	1.90	5	11%
MLT_OV($\alpha = 1.25$)	136	207	2.38	6	4%	284	297	4.27	5	<1%
MLT_OV($\alpha = 0.5$)	26	144	2.04	6	7%	150	162	1.61	5	17%
CGM	−80	105	1.08	6	37%	−114	165	1.41	5	23%
IRFM										
CM	−60	88	0.22	9	98%	−265	292	2.56	6	3%
MLT_noOV($\alpha = 1.25$)	−50	75	0.16	9	99%	−90	151	0.69	6	63%
MLT_noOV($\alpha = 0.5$)	−84	99	0.28	9	87%	−238	269	2.16	6	6%
MLT_OV($\alpha = 1.25$)	224	258	1.87	9	5%	195	226	1.54	6	18%
MLT_OV($\alpha = 0.5$)	93	124	0.43	9	92%	28	140	0.59	6	71%
CGM	−59	88	0.22	9	98%	−250	281	2.36	6	4%
Hyades										
CM	21	190	0.92	31	59%	−99	215	1.19	33	21%
MLT_noOV($\alpha = 1.25$)	25	189	0.92	31	59%	101	237	1.45	33	4%
MLT_noOV($\alpha = 0.5$)	−43	205	1.08	31	35%	−90	225	1.31	33	12%
MLT_OV($\alpha = 1.25$)	329	370	3.53	31	<1%	387	431	4.80	33	<1%
MLT_OV($\alpha = 0.5$)	195	265	1.82	31	<1%	150	237	1.45	33	4%
CGM	21	170	0.75	31	87%	−84	200	1.03	33	42%

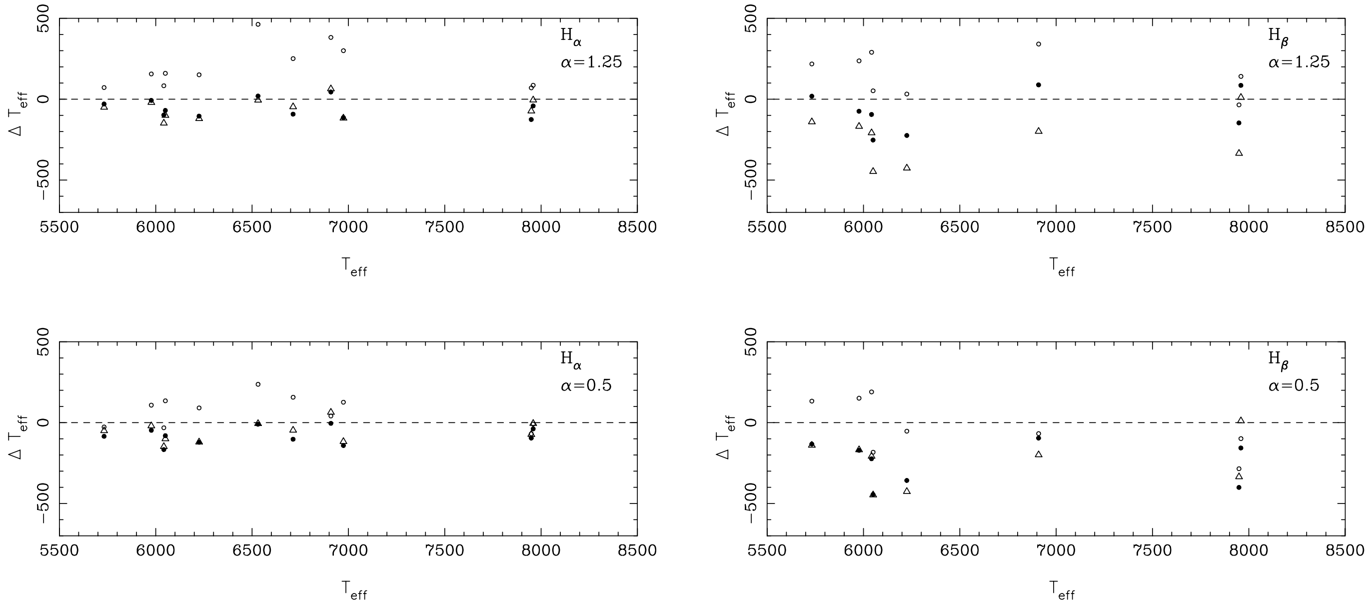

Fig. 5. Comparison between $T_{\rm eff}$ calculated from Balmer line profiles to those derived from the Infrared Flux Method. $\Delta T_{\rm eff} = T_{\rm eff}(\rm Balmer) - T_{\rm eff}(\rm IRFM)$. The triangles are results using the CM model, the filled circles are using the MLT with no overshooting and the open circles are those using MLT with overshooting. Notice that the H_β profile has given lower values of $T_{\rm eff}$ in general than H_α.

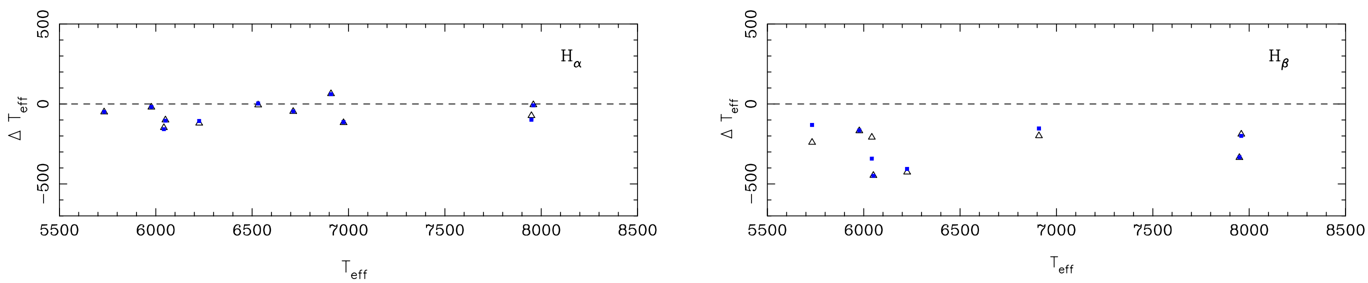

Fig. 6. Comparison between $T_{\rm eff}$ calculated from Balmer line profiles to those derived from the Infrared Flux Method. $\Delta T_{\rm eff} = T_{\rm eff}(\rm Balmer) - T_{\rm eff}(\rm IRFM)$. The triangles are results using the CM model, the filled squares are using the CGM model.

It is also useful to present the $T_{\rm eff}$ of the Hyades stars calculated by the Balmer line method for future reference.

The results are shown in Figs. 7 and 8 and Tables 6 and 7.

The Hyades stars allow a trend to be seen due to the greater number of stars considered. The trend in the H_α results seen for the fundamental stars between $\sim$ 6000 and $\sim$ 9000 K as temperature increases, for the Balmer line method to give increasingly lower values of $T_{\rm eff}$ compared to Fundamental values is also seen in comparison to the Geneva photometry value. Above ~ 7750 K this slope becomes much steeper giving very low values for $T_{\rm eff}$. This seems to be a systematic trend, thus the statistics can not really represent valid performance indicators on their own. Due to the sharp fall off at high temperatures the statistics excluded stars with a Geneva photometry value ≥ 7900 K.

The H_β profiles do not show this trend up to 7750 K. However, above this temperature, values again become very low compared to Geneva photometry. These trends in the H_α and H_β profiles are not apparent at all in the IRFM stars (Figs. 5 and 6) but could be seen in the fundamental stars (Figs. 3 and 4). The CGM model gives results which agree very accurately with the Geneva photometry results for both H_α and H_β. Clearly none of the models yield H_α profiles in agreement with Geneva photometry at all values of $T_{\rm eff}$ in the region considered.

5. Discussion

5.1. Different trends for H_α compared to H_β

In general, for the CM and CGM theories, the H_α results are around 100–200 K higher than those from H_β at around 6000 K, but steadily decreasing to about 0–100 K at 7000–8000 K. Note, however, that the MLT_noOV(α=1.25) results for α CMi agree well with the fundamental value for both H_α and H_β. In fact, for the MLT_noOV(α=1.25), as can be seen in Fig. 9, the H_α results are fairly consistent or higher than H_β at $T_{\rm eff}$ between 6000–7000 K, but over 7000 K H_β results are around 100–250 K higher than the H_α. Also for $T_{\rm eff} \leq 6000\ K$ H_β results are around 100–250 K higher than the H_α. However, if the mix-

Table 4. $T_{\rm eff}$ for IRFM stars from H_α profiles

	IRFM Stars				CM		MLT_noOV				MLT_OV				CGM	
							α = 1.25		α = 0.5		α = 1.25		α = 0.5			
HR	$v \sin i$	[M/H]	$T_{\rm eff}$	$\log g$	$T_{\rm eff}$	$\Delta T_{\rm eff}$	$T_{\rm eff}$	$\Delta T_{\rm eff}$	$T_{\rm eff}$	$\Delta T_{\rm eff}$	$T_{\rm eff}$	$\Delta T_{\rm eff}$	$T_{\rm eff}$	$\Delta T_{\rm eff}$	$T_{\rm eff}$	$\Delta T_{\rm eff}$
269	80	+0.03	7959	3.82	7954	−5	7917	−42	7920	−39	8045	86	7950	-9	7950	−9
343	100	+0.14	7949	3.91	7876	−73	7823	−126	7853	−96	8019	70	7880	-69	7850	−99
937	8	+0.03	6042	4.50	5894	−148	5944	−98	5875	−167	6125	83	6010	-32	5884	−158
996	8	+0.04	5732	4.45	5682	−50	5702	−30	5647	−85	5804	72	5705	-27	5682	−50
1101	8	−0.13	5977	3.98	5957	−20	5969	−8	5929	−48	6133	156	6085	108	5958	−19
1676	63	+0.08	6909	3.14	6973	64	6953	44	6904	−5	7291	382	6950	41	6970	61
2852	83	−0.18	6974	4.11	6857	−117	6860	−114	6832	−142	7274	300	7100	126	6860	−114
2930	60	−0.23	6531	3.34	6525	−6	6550	19	6521	−10	6994	463	6768	237	6534	3
7469	7	−0.17	6713	4.40	6666	−47	6620	−93	6610	−103	6964	251	6870	157	6667	−46
8665	9	−0.33	6225	4.10	6105	−120	6120	−105	6103	−122	6376	151	6316	91	6118	−107
8905	60	+0.06	6050	3.61	5950	−100	5980	−70	5969	−81	6210	160	6185	135	5945	−105

Table 5. $T_{\rm eff}$ for IRFM stars from H_β profiles

	IRFM Stars				CM		MLT_noOV				MLT_OV				CGM	
							α = 1.25		α = 0.5		α = 1.25		α = 0.5			
HR	$v \sin i$	[M/H]	$T_{\rm eff}$	$\log g$	$T_{\rm eff}$	$\Delta T_{\rm eff}$	$T_{\rm eff}$	$\Delta T_{\rm eff}$	$T_{\rm eff}$	$\Delta T_{\rm eff}$	$T_{\rm eff}$	$\Delta T_{\rm eff}$	$T_{\rm eff}$	$\Delta T_{\rm eff}$	$T_{\rm eff}$	$\Delta T_{\rm eff}$
269	80	+0.03	7959	3.82	7970	11	8044	85	7802	−157	8100	141	7860	−99	7979	20
343	100	+0.14	7949	3.91	7614	−335	7802	−147	7548	−401	7914	−35	7664	−285	7616	−333
937	8	+0.03	6042	4.50	5834	−208	5947	−95	5818	−224	6332	290	6232	190	5850	−192
996	8	+0.04	5732	4.45	5592	−140	5750	18	5599	−133	5950	218	5865	133	5601	−131
1101	8	−0.13	5977	3.98	5809	−168	5902	−75	5808	−172	6214	237	6128	151	5811	−166
1676	63	+0.08	6909	3.14	6710	−199	6997	88	6813	−96	7250	341	6841	−68	6756	−153
8665	9	−0.33	6225	4.10	5799	−426	6000	−225	5867	−358	6257	32	6172	−53	5819	−406
8905	60	+0.06	6050	3.61	5603	−447	5797	−253	5605	−445	6102	52	5867	−183	5600	−450

ing length parameter α is reduced to 0.5, the temperatures derived from the H_β profiles will be in the order of 200 K lower, thus agreeing with the results from H_α for $T_{\rm eff} \leq 6000\ K$ and $\geq 7000\ K$. Thus it seems that different values of α are more appropriate dependent on the $T_{\rm eff}$ of the star in question. This seems intuitively reasonable as over ∼7000 K the convectively unstable region is in a narrow band in the atmosphere. However below this effective temperature the unstable region descends lower into the star and becomes larger in width while at the same time the H_α is formed closer to the convection zone. At $T_{\rm eff} \leq 6000\ K$ the top of the convection zone moves deeper inside the envelope such that the H_α is formed at a greater distance from it, just as for the hotter stars of our samples.

In van't Veer-Menneret & Megessier (1996) the method of Balmer line fitting was used on the two Am stars, τ UMa and 63 Tau and for completeness they also used the IRFM method on these stars and confirmed the results were consistent. They found that these methods yield temperatures lower than the previously determined values by around 300 K for stars with $T_{\rm eff}$ between 7000 K-7200 K, which agrees with the results presented here. They argued that Smalley & Dworetsky (1993) had previously overestimated $T_{\rm eff}$, because they had not used the H_α profile, only the H_β profile which is highly sensitive to the choice of mixing length. In van't Veer-Menneret (1996), the mixing length α needed to be reduced from 1.25 to 0.5 to get H_β to agree with H_α.

Here, again, possibilities to reduce the difference between the two lines, which may give an insight into the real explanation, include:

1. If the temperature stratification in the turbulence models was such there were lower temperatures where H_α is formed then the profiles would be broader for each temperature and thus when fitting to observed H_α profiles we would fit to a lower $T_{\rm eff}$. This would be in agreement with the H_β results.
2. Using $\alpha \geq$1.25 in the region $\sim 6000\ K < T_{\rm eff} < 7000\ K$ and α=0.5 for $T_{\rm eff} \geq 7000\ K$ and $T_{\rm eff} \leq 6000\ K$ would ensure that H_α and H_β results are more closely matched.

From Figs. 3,4,7 and 8, it has been seen that using the H_α line profile to determine temperatures there is a trend for all models that, as temperature increases, the method gives increasingly lower values of $T_{\rm eff}$ in comparison with previously determined values. This trend is not apparent for the H_β line (we will leave consideration of the region of $T_{\rm eff}$ over 8000 K until the next section).

5.2. Problem of Balmer line profiles of stars at high effective temperatures

In Figs. 1 and 7, the trend is seen of anomalously negative differences compared to fundamental values for stars in the region 8000–9000 K, then returning to close agreement for stars over

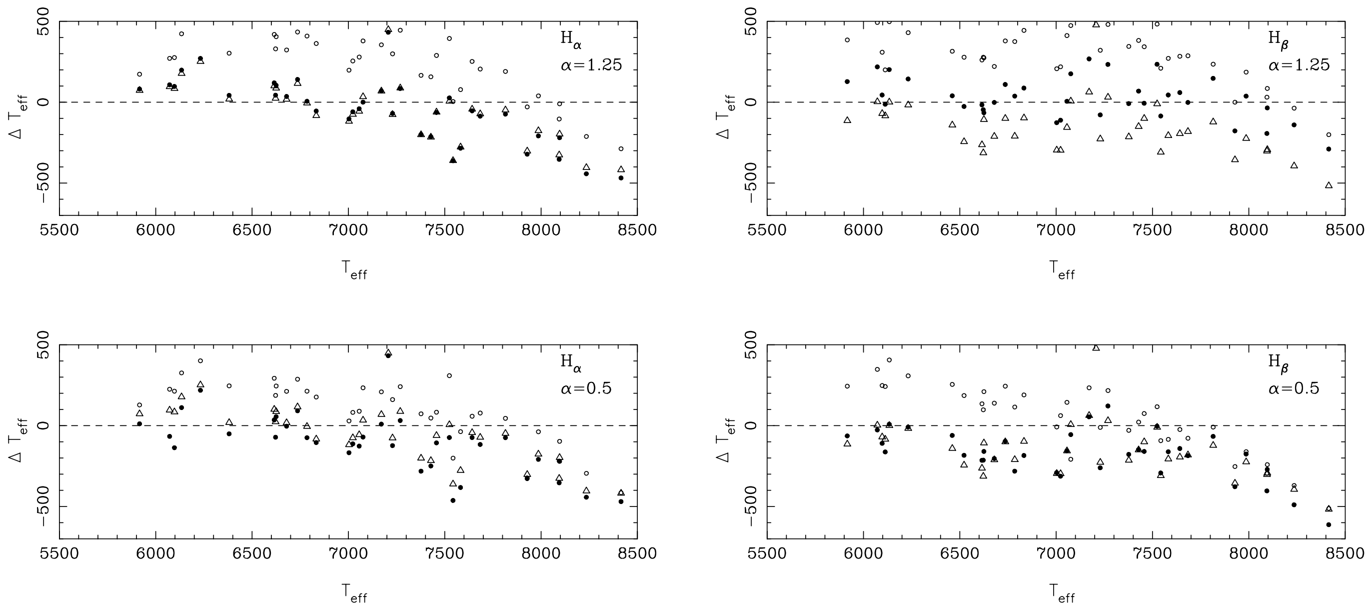

Fig. 7. Comparison between $T_{\rm eff}$ calculated from Balmer line profiles to those derived from Geneva photometry. $\Delta T_{\rm eff}$ = $T_{\rm eff}$(Balmer) - $T_{\rm eff}$(Geneva). The triangles are results using the CM model, the filled circles are using the MLT with no overshooting and the open circles are those using MLT_OV. Notice that the H_β profile has given lower values of $T_{\rm eff}$ in general than H_α. See results section for a detailed discussion.

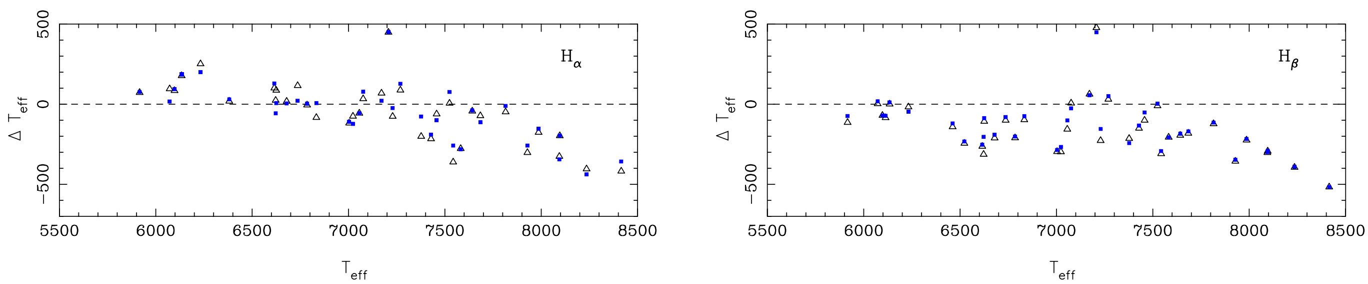

Fig. 8. Comparison between $T_{\rm eff}$ calculated from Balmer line profiles to those derived from Geneva photometry. $\Delta T_{\rm eff}$ = $T_{\rm eff}$(Balmer) - $T_{\rm eff}$(Geneva). The triangles are results using the CM model, the filled squares are using the CGM model. See results section for a detailed discussion.

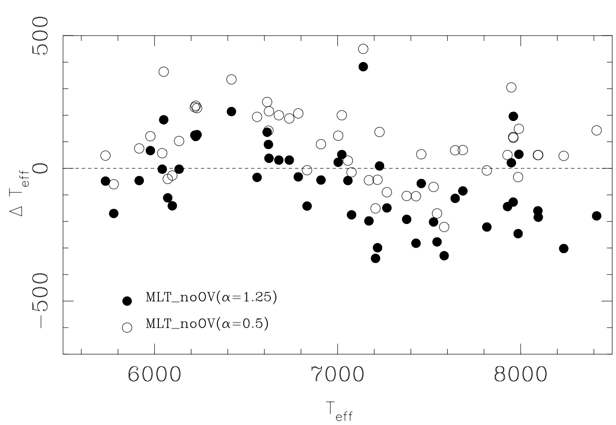

Fig. 9. The values of $T_{\rm eff}$ derived from the H_α line profile minus values derived from the H_β line for the stars considered in this paper. $\Delta T_{\rm eff} = T_{\rm eff}(H_\alpha) - T_{\rm eff}(H_\beta)$.

9000 K. Thus, it appears that none of the models considered here on their own predict the correct $T_{\rm eff}$ over the entire range of $T_{\rm eff}$. While it is true that at these higher effective temperatures the profile becomes sensitive to gravity, we would have to decrease the values of log g by around 0.4 dex to increase the temperatures determined to the fundamental values. This may be realistic considering the errors in the assumed values of log g vary between 0.3 and 0.5 dex. This would indicate a possible bias in previous methods to overestimate log g in this temperature region, if the synthesized Balmer profiles are accurate. This is entirely possible, as noted in Künzli et al. (1997) and in Paper I, where systematic effects for the gravity determination of main sequence stars in the Hyades with effective temperatures between 6500 and 8000 K were found.

This point is not dealt with further in this paper but work is currently being started which suggests that using two-component model atmospheres, which include a 'hot' and 'cold' temperature at each depth, work considerably better in this region.

Alternatively, there may be some other unidentified effect on Balmer line profiles in this temperature region.

Table 6. $T_{\rm eff}$ for Hyades stars from H_α

Hyades Stars					CM		MLT_noOV				MLT_OV				CGM	
							α = 1.25		α = 0.5		α = 1.25		α = 0.5			
HD	$v\sin i$	[M/H]	$T_{\rm eff}$	$\log g$	$T_{\rm eff}$	$\Delta T_{\rm eff}$	$T_{\rm eff}$	$\Delta T_{\rm eff}$	$T_{\rm eff}$	$\Delta T_{\rm eff}$	$T_{\rm eff}$	$\Delta T_{\rm eff}$	$T_{\rm eff}$	$\Delta T_{\rm eff}$	$T_{\rm eff}$	$\Delta T_{\rm eff}$
20430	3	+0.07	6072	4.45	6168	96	6179	107	6005	−67	6343	271	6297	225	6089	17
24357	50	−0.01	7023	4.27	6948	−75	6963	−60	6910	−113	7278	255	7105	82	6900	−123
25102	50	+0.11	6625	4.33	6712	87	6729	104	6680	55	7030	405	6870	245	6632	7
25825	0	+0.14	5916	4.49	5989	73	5997	81	5927	11	6089	173	6044	128	5992	76
26015	25	+0.16	6736	4.32	6852	116	6876	140	6827	91	7170	434	7023	287	6757	21
26345	18	+0.08	6679	4.32	6697	18	6712	35	6675	−4	7002	323	6891	212	6684	5
26462	0	−0.03	7003	4.27	6885	−118	6899	−104	6835	−168	7201	198	7032	29	6893	−110
26737	68	−0.09	6615	4.33	6716	101	6734	119	6650	35	7034	419	6908	293	6744	129
26784	6	+0.02	6134	4.43	6312	178	6332	198	6245	111	6557	423	6460	326	6321	187
26911	0	+0.22	6785	4.31	6780	−5	6790	5	6710	−75	7194	409	6998	213	6788	3
27176	125	+0.04	7428	4.23	7212	−216	7214	−214	7175	−250	7585	157	7475	47	7238	−190
27397	100	+0.09	7377	4.23	7176	−201	7177	−200	7095	−282	7543	166	7450	73	7300	−77
27406	10	+0.05	6097	4.44	6182	85	6000	97	5960	−137	6373	276	6310	213	6191	94
27429	150	+0.13	6833	4.30	6750	−83	6778	−55	6728	−105	7196	363	7010	177	6840	7
27459	68	+0.10	7524	4.22	7530	6	7556	26	7450	−74	7918	394	7833	309	7600	76
27628	25	+0.15	7171	4.25	7240	69	7240	69	7180	9	7526	355	7380	209	7192	21
27819	43	+0.12	8096	4.16	7899	−197	7876	−220	7875	−221	8086	−10	7999	−97	7900	−196
27934	87	+0.03	8235	4.14	7831	−404	7792	−443	7792	−443	8023	−212	7940	−295	7797	−438
27946	175	+0.06	7582	4.22	7305	−277	7297	−285	7199	−383	7660	78	7545	−37	7300	−282
28226	93	+0.15	7269	4.24	7357	88	7353	84	7300	31	7714	445	7510	241	7396	127
28294	135	+0.00	7056	4.26	7000	−56	7015	−41	6929	−127	7335	279	7145	89	7000	−56
28319	105	+0.07	7928	4.19	7626	−302	7606	−322	7600	−328	7899	−29	7605	−323	7670	−258
28355	93	+0.18	7815	4.20	7767	−48	7741	−74	7740	−75	8005	190	7860	45	7804	−11
28485	150	+0.13	7076	4.26	7110	34	7076	0	7005	−71	7455	379	7310	234	7154	78
28483	18	+0.14	6381	4.37	6400	19	6423	42	6330	−51	6684	303	6627	246	6411	30
28527	88	+0.14	7986	4.18	7810	−176	7777	−209	7777	−209	8025	39	7948	−38	7833	−153
28546	31	+0.25	7642	4.21	7599	−43	7588	−54	7568	−74	7894	252	7700	58	7604	−39
28556	140	+0.06	7457	4.23	7396	−61	7393	−64	7350	−107	7746	289	7540	83	7357	−100
28911	40	+0.03	6622	4.33	6646	24	6665	43	6550	−72	6952	330	6809	187	6565	−57
29375	155	+0.03	7229	4.24	7153	−76	7159	−70	7105	−124	7528	299	7390	161	7205	−24
29388	104	+0.06	8415	4.10	7997	−418	7946	−469	7945	−470	8127	−288	8000	−415	8057	−358
29488	154	+0.03	8094	4.16	7768	−326	7740	−354	7740	−354	7990	−104	7875	−219	7749	−345
30210	63	+0.37	7218	4.24	7856	638	7827	609	7825	607	8084	866	8014	796	7775	557
30738	12	+0.05	6232	4.40	6484	252	6502	270	6450	218	6761	529	6633	401	6432	200
30780	151	+0.11	7684	4.21	7612	−72	7597	−87	7567	−117	7889	205	7762	78	7572	−112
33254	13	+0.34	7207	4.24	7656	449	7639	432	7639	432	7947	740	7810	603	7657	450
28052	193	+0.08	7543	4.22	7182	−361	7180	−363	7080	−463	7547	4	7342	−201	7285	−258

$T_{\rm eff}$ 7000 K, log g 4.0 and a MLT_noOV model with $T_{\rm eff}$ = 7250 K, log g 4.0

5.3. *Differences between models*

As discussed in Sect. 3, and shown in Figs. 1 and 2, for H_α the CM and MLT_noOV(α=1.25) profiles are close. For H_β they are different as formed at different depths in the atmosphere, and the MLT_noOV(α=1.25) profile which matches an observed profile has a higher $T_{\rm eff}$.

Fig. 10 shows examples of HR343 showing clearly that the MLT_noOV and MLT_OV with α=1.25 shape fits the observations very well at the given values of log g; however the shape of the CM, CGM and MLT with α=0.5 is too broad. The CM profiles imitate the effect of using too high a log g, requiring, in each case, a decrease of log g to ∼3.5 dex from the one used of 3.91. However this is only an example of one star, and for other stars it is equally clear that the CM shape fits very well to that of the observation and that the MLT_noOV and MLT_OV with α=1.25 models gave profiles which were too high in the wings. No clear trend with temperature could be identified, thus we can not make any conclusions about the accuracy of the models from the shape alone.

6. Conclusion

We find that the results of $T_{\rm eff}$ from the H_α and H_β lines are different, which is consistent with the differing depths of formation of the lines. Differences of up to 400 K in the best fit $T_{\rm eff}$ are found between the four models of convection. The

Table 7. $T_{\rm eff}$ for Hyades stars from H_β

Hyades Stars					CM		MLT_noOV				MLT_OV				CGM	
							α = 1.25		α = 0.5		α = 1.25		α = 0.5			
HD	$v\sin i$	[M/H]	$T_{\rm eff}$	$\log g$	$T_{\rm eff}$	$\Delta T_{\rm eff}$	$T_{\rm eff}$	$\Delta T_{\rm eff}$	$T_{\rm eff}$	$\Delta T_{\rm eff}$	$T_{\rm eff}$	$\Delta T_{\rm eff}$	$T_{\rm eff}$	$\Delta T_{\rm eff}$	$T_{\rm eff}$	$\Delta T_{\rm eff}$
20430	3	+0.07	6072	4.45	6075	3	6290	218	6045	−27	6565	493	6420	348	6090	18
24357	50	−0.01	7023	4.27	6726	−297	6911	−112	6710	−313	7242	219	7085	62	6756	−267
25102	50	+0.11	6625	4.33	6518	−107	6691	−66	6465	−160	6899	274	6835	210	6538	−87
25825	0	+0.14	5916	4.49	5802	−114	6043	127	5852	−64	6301	385	6160	244	5842	−74
26015	25	+0.16	6736	4.32	6636	−100	6845	109	6639	−97	7115	379	6980	244	6656	−80
26345	18	+0.08	6679	4.32	6468	−211	6681	−2	6475	−204	6900	221	6818	139	6488	−191
26462	0	−0.03	7003	4.27	6707	−296	6876	−127	6712	−291	7210	207	6995	−8	6717	−286
26737	68	−0.09	6615	4.33	6352	−263	6598	−17	6400	−215	6876	261	6750	135	6362	−253
26784	6	+0.02	6134	4.43	6135	1	6335	201	6142	8	6632	498	6540	406	6145	11
26911	0	+0.22	6785	4.31	6575	−210	6822	37	6503	−282	6410	375	6900	115	6583	−202
27176	125	+0.04	7428	4.23	7278	−150	7496	68	7280	−148	7810	382	7450	22	7295	−133
27383	18	+0.07	6113	4.43	6029	−84	6100	−13	5950	−163	6313	200	6355	242	6040	−73
27397	100	+0.09	7377	4.23	7163	−214	7369	−9	7199	−178	7722	345	7348	−29	7134	−243
27406	10	+0.05	6097	4.44	6027	−70	6141	44	5987	−110	6406	309	6345	248	6027	−70
27429	150	+0.13	6833	4.30	6736	−97	6920	87	6735	−185	7277	444	7023	190	6758	−75
27459	68	+0.10	7524	4.22	7514	−10	7758	234	7520	−4	8003	483	7641	117	7527	3
27628	25	+0.15	7171	4.25	7234	63	7438	267	7225	54	7810	639	7405	234	7227	56
27534	40	−0.02	6522	4.35	6278	−244	6495	−27	6338	−184	6800	278	6708	186	6289	−233
27483	18	+0.17	6461	4.36	6320	−141	6500	39	6400	−61	6776	315	6716	255	6341	−120
27819	43	+0.12	8096	4.16	7803	−293	8060	−36	7825	−271	8181	85	7855	−241	7806	−290
27934	87	+0.03	8235	4.14	7841	−394	8094	−141	7745	−490	8198	−37	7865	−370	7844	−391
27946	175	+0.06	7582	4.22	7376	−206	7626	44	7420	−162	7853	271	7497	−85	7375	−207
28226	93	+0.15	7269	4.24	7300	31	7502	233	7390	121	7750	481	7486	217	7319	50
28294	135	+0.00	7056	4.26	6900	−156	7061	5	6900	−156	7468	412	7200	144	6955	−101
28319	105	+0.07	7928	4.19	7572	−356	7750	−178	7550	−378	7928	0	7675	−253	7581	−347
28355	93	+0.18	7815	4.20	7693	−122	7962	147	7748	−67	8050	235	7806	−9	7700	−115
28485	150	+0.13	7076	4.26	7083	7	7251	175	7020	−56	7550	474	7342	−208	7050	−26
28527	88	+0.14	7986	4.18	7762	−224	8023	37	7810	−176	8172	186	7825	−161	7769	−217
28546	31	+0.25	7642	4.21	7448	−194	7701	59	7500	−142	7926	284	7618	−24	7458	−184
28556	140	+0.06	7457	4.23	7357	−100	7450	−7	7297	−160	7800	343	7532	75	7405	−52
28911	40	+0.03	6622	4.33	6309	−313	6575	−47	6408	−214	6900	278	6720	98	6318	−204
29375	155	+0.03	7229	4.24	7002	−227	7150	−79	6968	−261	7550	321	7218	−11	7074	−155
29388	104	+0.06	8415	4.10	7898	−517	8125	−290	7802	−613	8214	−201	7903	−512	7898	−517
29488	154	+0.03	8094	4.16	7792	−302	7900	−194	7690	−404	8125	31	7799	−295	7795	−299
30210	63	+0.37	7218	4.24	7805	587	8126	908	7868	650	8259	1041	7900	682	7814	596
30738	12	+0.05	6232	4.40	6184	−17	6375	143	6223	−9	6662	430	6540	308	6185	−47
30780	151	+0.11	7684	4.21	7503	−181	7682	−2	7498	−186	7971	287	7606	−78	7514	−170
33254	13	+0.34	7207	4.24	7685	478	7978	771	7790	583	8201	994	7765	558	7656	449
28052	193	+0.08	7543	4.22	7234	−309	7457	−86	7250	−293	7753	210	7450	−93	7250	−293

tests are inconclusive between the four models, however the MLT_noOV and the CM and CGM models all give similarly reasonable results and perform better than MLT_OV consistent with the results with $uvby$ photometry in Paper I. The improvement to the CM model, the CGM model, has been slightly more successful in predicting $T_{\rm eff}$. We find for the mixing length theory, it seems appropriate to set $\alpha \geq 1.25$ in the region $6000\ K < T_{\rm eff} < 7000\ K$ but need α=0.5 in the two regions $T_{\rm eff} \leq 6000\ K$ and $T_{\rm eff} \geq 7000\ K$.

High rotation and metallicity caused slight difficulties in modelling both Balmer line profiles and may be part of the systematic problems with the profiles. Although these effect H_β more than H_α as there are more metal lines in this wavelength region, the effect is expected to be <75 K at most, for a 0.1 dex change in metallicity.

Comparing model values of $T_{\rm eff}$ with fundamental values, which is the ideal test, the MLT_noOV is the most successful, although no model reproduces the observations very well and the conclusion is only based on a few stars. The main reason that MLT_noOV(α=1.25) model gives the best results overall is because more stars in our tests have a $T_{\rm eff}$ between 6000 and 7000 K, ie. in the region where this parameter should be set to α=1.25. The CM and CGM results are quite close to the MLT_noOV ones, though not quite as good. The MLT_OV model is clearly discrepant, as in Paper I, and can be ruled out as a sufficiently accurate theory of conditions in stellar atmo-

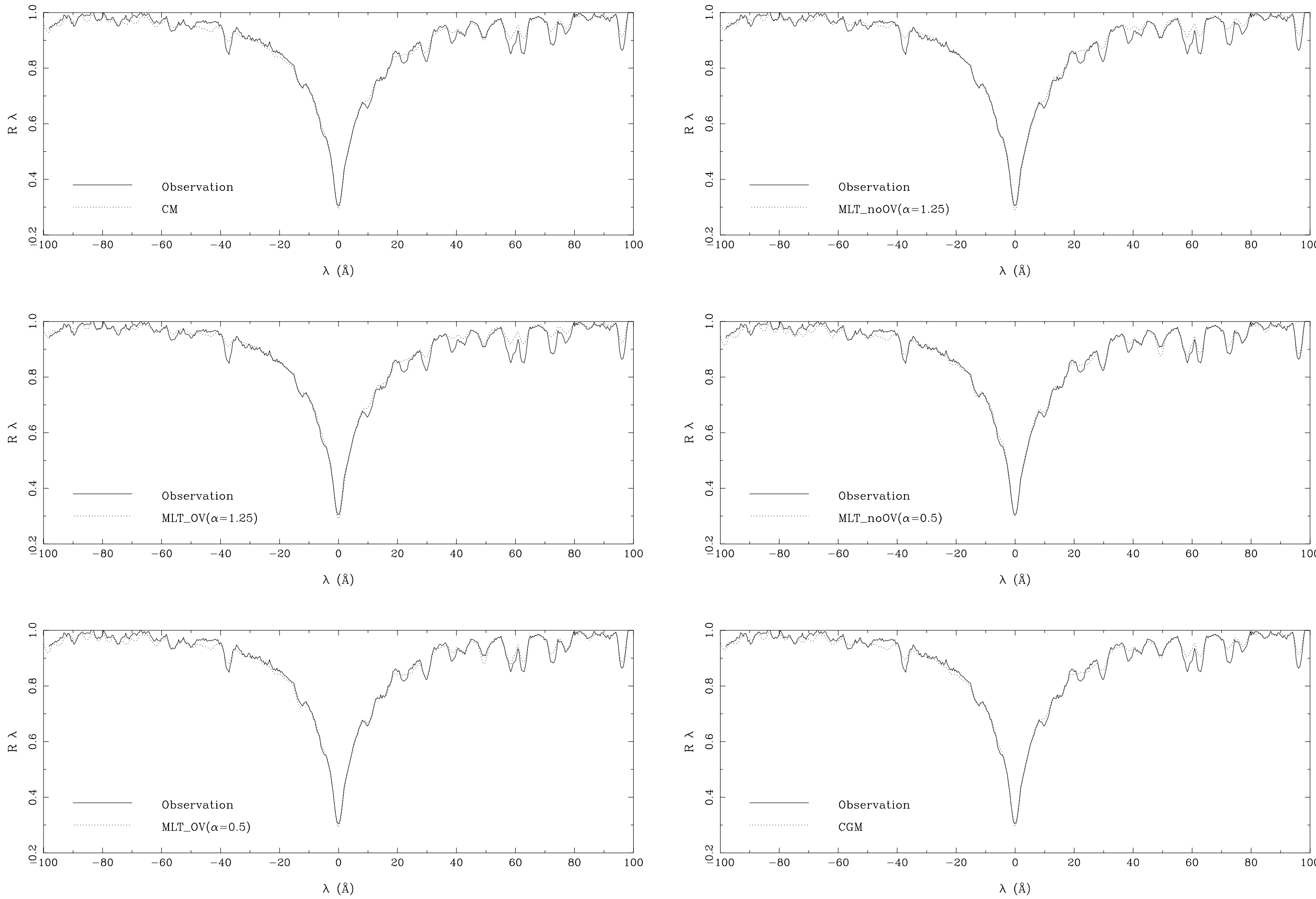

Fig. 10. Observations of the H_β profile of HR343, ($T_{\rm eff}$ from the Infrared Flux Method 7949 K) with the best fit model profiles. Notice the MLT_noOV(α=1.25) model profiles fit well however the CM and CGM profiles are too deep in the wings.

spheres. It predicts the profiles are formed at a higher level in the atmosphere, nearer the outer surface, than the other three models and this appears to be disproved by this model's poor results. However, because of the slopes of the H_α results for all the models, clearly there is a systematic problem with all the models. This slope is not apparent for H_β and thus may be connected with the H_α profile being formed above the convection zone. As the $T_{\rm eff}$ decreases, the convection zone becomes both deeper and closer to the region where the H_α profile is formed, but then for $T_{\rm eff} \leq 6000\ K$ the distance between this zone and H_α increases again. Whereas the H_β is formed within the convection zone at $T_{\rm eff} \leq 8000\ K$. At $T_{\rm eff} \geq 8500\ K$ convection becomes so insignificant as to not effect results.

An application of alternative broadening theories for Balmer line profiles to A and F stars could also be helpful (see Stehlé 1996)

In conclusion, the CM, CGM and MLT_noOV models (using α = 0.5 for the two regions $T_{\rm eff} \leq 6000$ K and $T_{\rm eff} \geq 7000$ K and $\alpha \geq 1.25$ in the region 6000 K $< T_{\rm eff} <$ 7000 K), all give similar results, performing reasonably well in predicting observations, however, show some systematic errors over the region 6000 K–10000 K.

Acknowledgements. The referee, Fiorella Castelli is thanked for her constructive comments on the original manuscript. This work has made use of the hardware and software provided at Keele by the PPARC Starlink Project and NASA's Astrophysics Data System Abstract Service. Rebecca Gardiner's PhD studentship is funded by EPSRC. Friedrich Kupka acknowledges support by the project *Convection in Stars*, grant P11882-PHY of the Austrian Fonds zur Förderung der wissenschaftlichen Forschung. We thank Claude van't Veer-Menneret for useful discussion and for providing her H_β spectrum of Procyon.

References

Bernacca P.L., Perinotto M., 1970, CoAsi 239, 1B
Berthet S., 1990, A&A 236, 440
Blackwell D.E., Lynas-Gray A.E., 1994, A&A 282, 899
Blackwell D.E., Shallis M.J., 1977, MNRAS 180, 177
Canuto V., Goldman I., Mazzitelli I., 1996, ApJ 473, 550
Canuto V., Mazzitelli I., 1991, ApJ 370, 295
Canuto V., Mazzitelli I., 1992, ApJ 389, 724
Castelli F., 1996. In: Adelman S.J., Kupka F., Weiss W.W. (eds.) Model Atmospheres and Spectrum Synthesis. A.S.P. Conf. Proc. 108, p. 85
Castelli F., Gratton R.G., Kurucz R.L., 1997, A&A 318, 841
Fuhrmann K., Axer M., Gehren T., 1993, A&A 271, 451
Fuhrmann K., Axer M., Gehren T., 1994, A&A 285, 585

Gray D.F., 1992, Obs. and Analysis of Stellar Photospheres, CUP
Hauck B., Mermilliod M., 1998, A&AS 129, 431
Kobi D., North P., 1990, A&AS 85, 999
Künzli M., North P., Kurucz R.L., Nicolet B., 1997, A&AS 122, 51
Kupka F., 1996 In: Adelman S.J., Kupka F., Weiss W.W. (eds.) Model Atmospheres and Spectrum Synthesis. A.S.P. Conf. Proc. 108, p. 73
Kurucz R.L., 1970, Smithsonian Ap. Obs. Spec. Rept., No. 309
Kurucz R.L., 1979a, ApJS 40, 1
Kurucz R.L., 1979b, Dudley Obs. Rept. 14, 271
Kurucz R.L., 1992, Rev. Mex. Astron. Astrofis. 23, 181
Kurucz R.L., 1993, Kurucz CD-ROM 13: ATLAS9, SAO, Cambridge, USA
Kurucz R.L., Bell B., 1995, Kurucz CD-ROM 23: Atomic Line List, SAO, Cambridge, USA
Kurucz R.L., Furenlid I., Brault J., Testerman L.,1984, Solar Flux Atlas from 296 to 1300nm, National Solar Obs., Sunspot
Mills D., Webb J., Clayton M., 1997, Starlink User Note 152.4
Nissen P.E., 1988, A&A 199, 146
Peterson D.M., 1969, Smithsonian Ap. Obs. Spec. Rept., No. 293
Smalley B., 1992, Ph.D. Thesis, University of London. Chap. 5
Smalley B., 1999, A&A, priv. comm.
Smalley B., Dworestsky M.M., 1993, A&A 271, 515
Smalley B., Dworestsky M.M., 1995, A&A 293, 446
Smalley B., Kupka F., 1997, A&A 328, 349 (Paper I)
Smalley B., Smith K.C., 1995, UCLSYN Userguide
Smith K.C., 1992, Ph.D. Thesis, University of London. Chap. 5
Smith K.C., van't Veer C., 1987, In: Adelman S.J., Lanz T. (eds.) Elemental Abundance Analyses. Institut d'Astronomie de l'Universite de Lausanne, p. 133
Steffen M., Ludwig H-G., 1999, In: Giminez A., Guinan E.F., Montesinos B. (eds.) Theory and Tests of Convection in Stellar Structure. A.S.P. Conf. Proc. 173, p. 217
Stehlé C., 1996, In: Adelman S.J., Kupka F., Weiss W.W. (eds.) Model Atmospheres and Spectrum Synthesis. A.S.P. Conf. Proc. 108, p. 56
van't Veer-Menneret C., 1996, In: Adelman S.J., Kupka F., Weiss W.W. (eds.) Model Atmospheres and Spectrum Synthesis. A.S.P. Conf. Proc. 108, p. 56
van't Veer-Menneret C., Megessier C., 1996, A&A 309, 879
Vidal C.R., Cooper J., Smith E.W., 1973, ApJS 25 37